

# Interferometric Studies of Low-Mass Protostars

Jes K. Jørgensen<sup>1</sup>

<sup>1</sup>Niels Bohr Institute & Centre for Star and Planet Formation, University of Copenhagen  
Juliane Maries Vej 30 DK-2100, Copenhagen Ø, Denmark  
email: jeskj@nbi.dk

**Abstract.** With the advances in high angular resolution (sub)millimeter observations of low-mass protostars, windows of opportunities are opening up for very detailed studies of the molecular structure of star forming regions on wide range of spatial scales. Deeply embedded protostars provide an important laboratory to study the chemistry of star formation – providing the link between dense regions in molecular clouds from which stars are formed, i.e., the initial conditions and the end product in terms of, e.g., disk and planet formation. High angular resolution observations at (sub)millimeter wavelengths provide an important tool for studying the chemical composition of such low-mass protostars. They for example constrain the spatial molecular abundance variations – and can thereby identify which species are useful tracers of different components of the protostars at different evolutionary stages. In this review I discuss the possibilities and limitations of using high angular resolution (sub)millimeter interferometric observations for studying the chemical evolution of low-mass protostars – with a particular keen eye toward near-future ALMA observations.

**Keywords.** astrochemistry — stars: formation — planetary systems: protoplanetary disks — ISM: abundances — ISM: molecules — radiative transfer — techniques: high angular resolution — techniques: interferometric

---

## 1. Introduction

Our standard picture suggests that low-mass stars form from the gravitational collapse of dense molecular cloud cores. In the earliest stages, the newly formed young star is deeply embedded in its infalling envelope of cold gas and dust obscuring its radiation. Eventually this envelope is dissipated revealing the pre-main sequence star surrounded by the circumstellar disk. From an astrochemical point of view, one of the prime goals is to understand how dust and gas evolves during this process – from the cold molecular clouds until it arrives in a planet-forming disk.

In this context, studies of young stars during their embedded (Class 0 and I) stages are of prime importance for our understanding of the formation of solar-type stars and their disks. On the one hand, they make it possible to probe the star formation process right after the collapse has occurred and thereby reveal the physical and chemical relationship between the protostar and the environment in which it forms. On the other hand, the initial conditions for the subsequent evolution of the young star are determined during these embedded stages. This is when the star accretes the bulk of its mass and a circumstellar disk forms. The physical and chemical structure of this disk may determine whether planets are formed around a given young star later in its evolution.

The evolution of the gas and dust during these stages is a complex process. It involves following the chemistry through environments with significantly varying physical properties (densities, temperatures); properties that are changing on time-scales that are relatively short or comparable to, e.g., the time-scales for molecules to freeze-out on dust

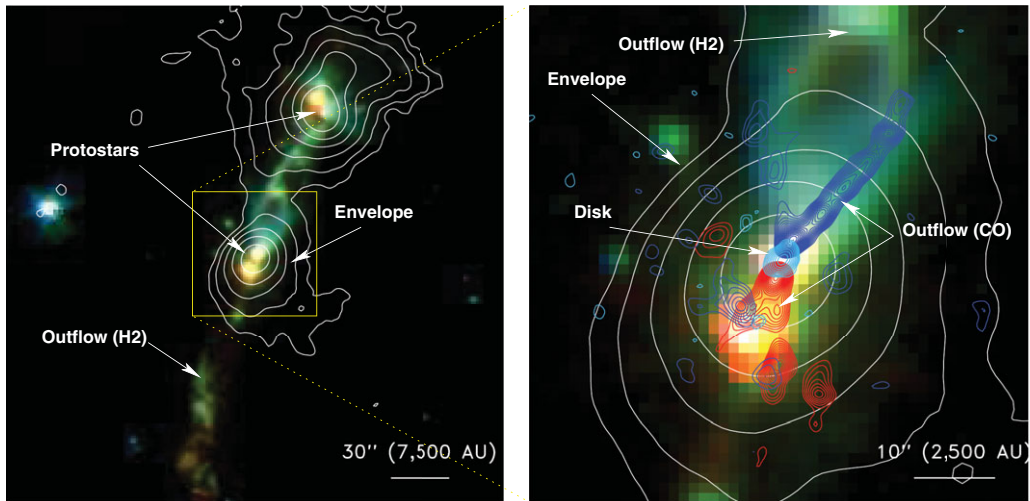


**Figure 1.** Observations of embedded protostars in the L1448 region with the Class 0 protostar L1448-C in the center of the picture. **The envelope** is revealed by its cold dust probed by JCMT/SCUBA 850  $\mu\text{m}$  continuum observations. **The outflow** is traced by Spitzer observations of shocked  $\text{H}_2$  at temperatures of 500–1000 K (green color in background image) and by SMA observations of  $\text{CO } J = 2-1$  emission at temperatures of 20–50 K (red and dark blue contours in right panel). **The disk** is revealed by SMA 850  $\mu\text{m}$  continuum observations (light-blue contours in right panel). Spitzer/IRAC observations from Jørgensen *et al.* (2006) (background image; blue is 3.6  $\mu\text{m}$ ; green 4.5  $\mu\text{m}$  and red 8.0  $\mu\text{m}$ ) and SMA and JCMT observations from Jørgensen *et al.* (2007).

grains, for grain-surface reactions in the dust grains' ice mantles or for gas-phase chemistry in the warm gas in the envelope. For a typical molecular cloud core, densities range from just  $10^3 - 10^4$  molecules  $\text{cm}^{-3}$  in the molecular cloud stage to  $10^7 - 10^8$   $\text{cm}^{-3}$  in the inner envelopes of low-mass protostars, and potentially even higher in their disks. Likewise, temperatures typically range from around 10 K in the outer envelopes to a few hundred K in the inner envelope or surface layers of the circumstellar disks – and can locally increase even further through shocks related to the accretion or caused by the ubiquitous outflows.

To fully understand the chemical evolution of low-mass protostars we therefore need to observe a wide range of spatial scales with observational techniques sensitive to these large variations in physical conditions. (Sub)millimeter interferometric observations provide such a unique opportunity to probe the warm and dense material in the innermost regions of protostellar systems – and to image the radial variations in the chemistry related to the changes in the underlying physical structures of the protostars and their environments.

## 2. Continuum studies of low-mass protostars

Continuum emission at (sub)millimeter wavelengths is dominated by thermal radiation from the dust grains in the envelopes and thus measure the combined effects of increasing temperatures and column densities toward the center of the protostellar cores. On larger ( $> 1000$  AU) scales, the temperature and density distributions of the protostellar envelopes can be determined from radiative transfer modeling of single-dish submillimeter continuum images and mid- and far-infrared spectral energy distributions of the young stellar objects (e.g., Jørgensen *et al.* 2002; Schöier *et al.* 2002; Shirley *et al.* 2002). Such radiative transfer models show that the bulk of the mass in typical infalling envelopes

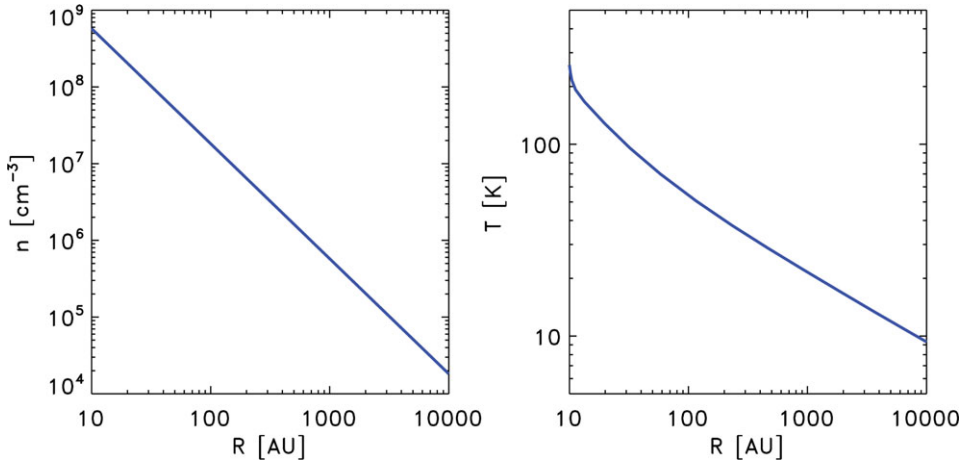


**Figure 2.** Density and temperature profile for  $1 M_{\odot}$  envelope around  $5 L_{\odot}$  protostar. The envelope is assumed to have a power-law density profile,  $n \propto r^{-1.5}$ , corresponding to material in free-fall toward the center, an inner radius of 10 AU and an outer radius of 10,000 AU. The temperature is calculated self-consistently using the DUSTY radiative transfer code (Ivezić *et al.* 1999; see also Jørgensen *et al.* 2002).

is located on large scales and that gas and dust heated to 20 K or more are located in the inner 1000 AU ( $5''$  at a typical distance of 200 pc for nearby low-mass star forming regions).

These types of profiles provide a good first order description of the physical conditions in the protostellar envelopes necessary to solve for excitation of molecules, predict line strengths and, e.g., calculate synthetic spectra that can be compared to observations to constrain molecular abundances or kinematics of low-mass protostars. However, it is worth noting that these are dependent on a number of underlying assumptions about among others (i) simplified structures of the sources, (ii) dust properties – in particular opacities that may vary as function of density, temperature and more, (iii) some degree of coupling between the dust and gas – e.g., in terms of the thermal balance.

### 2.1. Extrapolation of envelope structures to small radii

In recent years significant efforts have been put into characterizing the inner few hundred AU of embedded protostars through continuum observations at (sub)millimeter wavelengths. One of the expected outcomes of the collapse of rotating protostellar cores is the formation of a circumstellar accretion disk. Theoretically the growth of this disk is expected to be closely coupled to the rotation speed and infall rate in the initial core (Terebey *et al.* 1984) – as well as whether magnetic fields introduce differential rotation (e.g., Basu 1998).

At (sub)millimeter wavelengths the continuum emission from such disks is likely dominated by the thermal radiation from their dust grains, which is becoming stronger at shorter wavelengths with  $F_{\nu} \propto \nu^{2-3}$  or steeper. (Sub)millimeter interferometric observations of the continuum emission toward embedded protostars coupled to detailed radiative transfer models similar to those described above (e.g., Jørgensen *et al.* 2004a, 2005a, 2009; Brinch *et al.* 2007; Chiang *et al.* 2008; Lommen *et al.* 2008; Enoch *et al.* 2009, 2011) show evidence for compact continuum emission on  $\sim 1''$  scales (inner  $\sim 100$  AU) that cannot be explained by typical infalling envelopes (Fig. 3). If these compact continuum components indeed reflect the presence of circumstellar disks on  $\sim 100$  AU scales, this

would argue in favor of a scenario in which disks are formed early, and grow rapidly to sizes comparable to those around more evolved sources (e.g., Jørgensen *et al.* 2009; Enoch *et al.* 2011). But the compact continuum emission can also be explained by, e.g., magnetic pseudo-disks (e.g., Brinch *et al.* 2009; Maury *et al.* 2010), i.e., flattened disk-like structures that extend out to 500–1000 AU scales, but are not rotationally supported (Galli & Shu 1993a,b; Hennebelle & Ciardi 2009), or by magnetic accretion shock walls (Chiang *et al.* 2008).

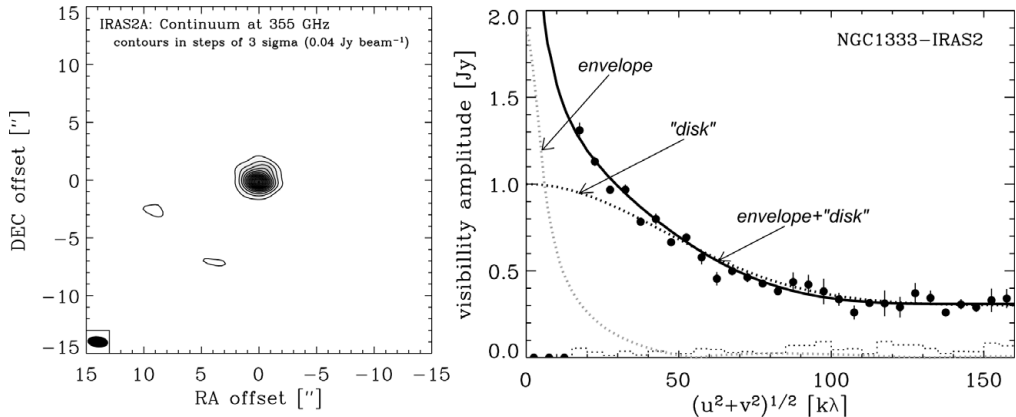


**Figure 3.** SMA 850  $\mu\text{m}$  continuum observations from the deeply embedded (Class 0) protostar NGC1333-IRAS2A (Jørgensen *et al.* 2005a). **Left:** image at 355 GHz. **Right:** visibility amplitude as function of projected baselines probing scales from about 20'' to 1'' (2000 AU to 100 AU radius). The results of dust radiative transfer modeling of the sources are also shown: a model with a pure envelope (explaining the larger-scale SCUBA emission and single-dish line observations of the collapsing core on scales from a few thousand to 10,000 AU) cannot account for most of the emission seen with the SMA, but with a compact continuum component ("disk") introduced the emission is well-reproduced on all scales.

In more evolved protostars, some of these compact continuum components can unambiguously be attributed to Keplerian disks through resolved line observations revealing their kinematical structures (e.g., Brinch *et al.* 2007; Lommen *et al.* 2008; Jørgensen *et al.* 2009). However, for the more embedded sources with envelope masses larger than about 0.1  $M_{\odot}$ , the key (sub)millimeter transitions of species such as CO, HCO<sup>+</sup>, CS, and HCN, traditionally used for studying low-mass protostars, become optically thick on few hundred AU scales and are thus not able to probe the region where rotation starts to dominate over infall. This lack of kinematical information makes the interpretation of the compact continuum structures unclear. One option is instead to target the isotopologues of the same molecular species: in fact, for one of the best studied Class 0 protostars, NGC 1333-IRAS2A, high angular SMA observations of the H<sup>13</sup>CN isotopologue actually suggest that the kinematics of the envelope is dominated by infall rather than rotation down to few hundred AU scales (Brinch *et al.* 2009) – perhaps evidence for the pseudo-disk interpretation. Generally, however, the current interferometers have lacked the sensitivity to image the emission from low surface brightness emission from these isotopologues and such studies are consequently sparse.

No matter the physical nature of the compact continuum components, the main issue raised by these observations is that the profiles of low-mass protostars remain poorly constrained on  $\sim 100$  AU scales. They illustrate that extrapolations of density profiles

established on a few thousand AU scales are problematic and absolute abundances of molecular species measured relative to such density profiles – either through high excitation transitions or in resolved observations – should be taken with care when used for interpretations of the chemical structures of protostars. Another solution is to consider relative abundances of different molecular species that can be resolved spatially, although for this differences in the chemical structures of the studied molecules (e.g., radial variations) should be taken into account. Comparing, e.g., the (sub)millimeter rotational transitions from molecules such as CO that are thought to desorb at temperatures of 20–30 K to molecules only thought to be present in much warmer gas will likewise be strongly model dependent.

### 3. Interferometric observations of the gas chemistry of low-mass protostars

As for the continuum observations there are definite benefits of going to the shorter submillimeter wavelengths when studying low-mass protostars. Interpretation of lower excitation lines are complicated by the fact that a large fraction of their emission may arise in the outer cold regions of the envelopes, where the lines can also become optically thick. As an example, Fig. 4 compares the radius where the  $\tau = 1$  surface is encountered for continuum and HCO<sup>+</sup> 3–2 line emission (calculated from the outside inwards) in spherical, free-falling envelopes (density profile,  $n \propto r^{-1.5}$ ) and a singular isothermal spheres ( $n \propto r^{-2}$ ) of differing masses. As shown in the figure, for typical low-mass protostars the continuum emission remains optically thin down to scales of a few AU even for steep density profiles and massive envelopes. In contrast, the line emission of a commonly used tracer such as HCO<sup>+</sup> 3–2 becomes optically thick at radii  $> 100$  AU even for envelopes of a few  $0.1 M_{\odot}$  mass. This means that the continuum optical thickness will not obscure the line radiation and that it, at least from this perspective, should be possible to find molecular species tracing the center regions of these protostars. However, many of the more common molecular species traditionally targeted using (sub)millimeter interferometry are not sensitive to what is going on the smallest scales – for example, making observations of the kinematics of the inner rotating and infalling regions of the protostellar envelopes and disks difficult (see also Jørgensen *et al.* 2009).

#### 3.1. Radial chemical variations in envelopes: large to intermediate scales

As noted above, the chemistry in protostellar environments is thought to evolve on time-scales similar to the dynamical time-scales for the protostellar envelopes. For example, freeze-out of molecules such as CO onto dust grains is expected to occur over time-scales of  $10^4 - 10^5$  years at the densities characterizing the outer ( $T < 20 - 30$  K) envelope (e.g., Jørgensen *et al.* 2005b). As the material is falling-in toward the center of the cores, the molecular species will evaporate back into the gas-phase as the temperature due to heating by the central protostar exceeds the desorption temperature for the ices (typically 20–30 K for CO, 90–100 K for water containing ices etc.).

Based on line radiative transfer modeling of single-dish observations of protostellar envelopes Jørgensen *et al.* (2004b, 2005b) suggested that molecules such as CO and related species would show characteristic “drop abundance” profiles. That is, an outer envelope with a small degree of depletion because of the low densities and associated long time-scales for freeze-out, an intermediate region where the density is high enough that significant depletion can occur, but the temperature is low enough to avoid thermal desorption and an inner region where the molecules desorb back into the gas-phase due to higher temperatures (see, e.g., middle panel in right column of Fig. 5). The validity of

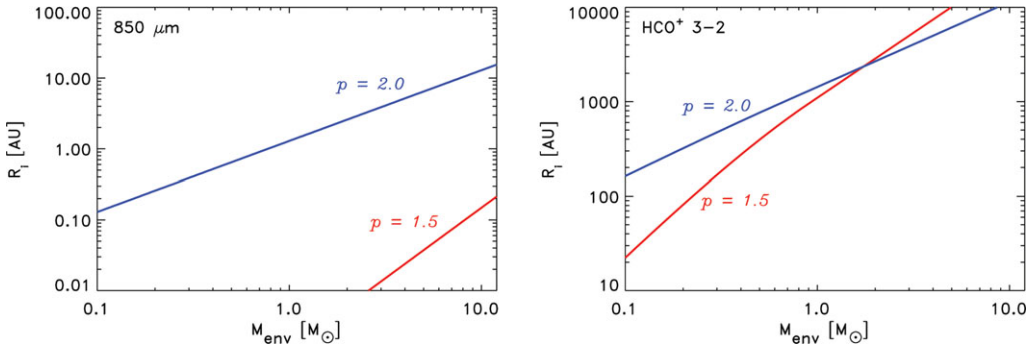


**Figure 4.** Radius where the  $\tau = 1$  surface is reached for emission from continuum at  $850 \mu\text{m}$  (left) and the  $\text{HCO}^+$  3–2 line (right) as function of envelope mass. Note the differences in scales of the Y-axes. In each plot two curves are shown for envelopes with density profiles of  $n \propto r^{-1.5}$  and  $n \propto r^{-2}$ , respectively. For  $\text{HCO}^+$  the optical depth was calculated using the Radex escape probability code (van der Tak *et al.* 2007) assuming a temperature of 25 K, density of  $5 \times 10^5$ ,  $\text{HCO}^+$  abundance with respect to  $\text{H}_2$  of  $10^{-9}$  and line width of  $3 \text{ km s}^{-1}$  typical values observed for the envelopes of low-mass protostars. The optical depth is only weakly dependent on the density and temperature in this regime, but naturally increases with increasing abundance and decreasing line width.

this scenario (in particular, the presence of the “intermediate” and “inner” regions”) can be tested by direct imaging of different molecular species and by constraining their radial abundance variations. Fig. 5, as an example, compares the radial profiles (distribution of visibility amplitudes as function of projected baselines) for three molecular species, SO,  $\text{H}^{13}\text{CN}$  and  $\text{CH}_3\text{OH}$ , toward the Class 0 protostar, NGC 1333-IRAS2A (compare also to Fig. 3). The three species show significantly different emission morphologies: SO is well reproduced by a constant abundance throughout the envelope and any abundance enhancement on small-scales can be ruled out. The emission of  $\text{H}^{13}\text{CN}$  cannot be explained by a constant abundance, but rather require a drop in abundance similar to the profiles described above.  $\text{CH}_3\text{OH}$  finally shows compact emission that can best be described as originating in either the circumstellar disk or in the inner warm envelope – or “hot corino”.

The freeze-out and desorption of molecules also play an important role in regulating the gas-phase chemistry in different regions of the protostellar envelopes. Perhaps the simplest example is the chemistry of the key molecular ion  $\text{N}_2\text{H}^+$ .  $\text{N}_2\text{H}^+$  is strongly regulated by the presence or absence of CO: when CO is present in the gas-phase it acts as the main destroyer of  $\text{N}_2\text{H}^+$ , lowering its abundance significantly driving nitrogen into  $\text{N}_2$ . However, when CO is starting to freeze-out, the abundance of  $\text{N}_2\text{H}^+$  is enhanced (e.g., Jørgensen *et al.* 2004b, and references therein). Again, this and similar effects can be tested through imaging of emission from CO and  $\text{N}_2\text{H}^+$  at millimeter wavelengths. Fig. 6 shows one example for the L483 protostellar cores (Jørgensen 2004); similar morphologies have been observed toward Barnard 1c (Matthews *et al.* 2006) and IRAS 16293-2422 (Jørgensen *et al.* 2011).

### 3.2. The innermost regions: hot corinos and disks

One of the most interesting recent developments in the astrochemistry of low-mass protostars has undoubtedly been the detections on complex organics in low-mass protostars (Cazaux *et al.* 2003; Bottinelli *et al.* 2004; Sakai *et al.* 2006). A parallel has been proposed between these “hot corinos” and the high-mass protostellar “hot cores” related to the evaporation of icy-mantles on scales where the dust and gas is heated to

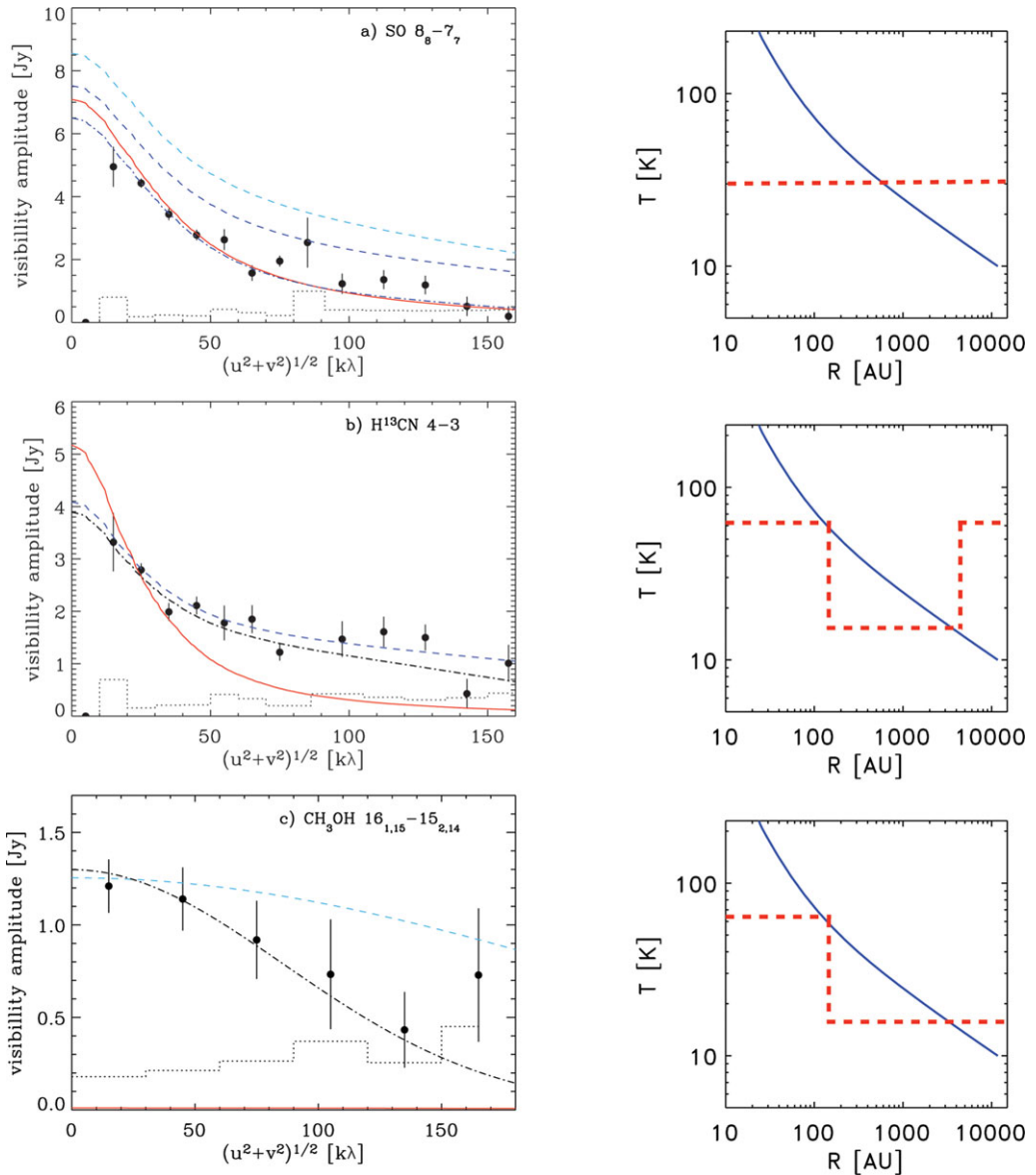


**Figure 5.** Abundance profiles for three different molecular species (SO,  $\text{H}^{13}\text{CN}$  and  $\text{CH}_3\text{OH}$  in the top, middle and bottom panels, respectively) toward the Class 0 protostar NGC 1333-IRAS2A imaged with the SMA (Jørgensen *et al.* 2005a). The **left column** shows the visibility amplitudes (averaged in the spectral domain over the line profile) as function of projected baseline length. The error bars indicate  $1\sigma$  errors and the dotted histogram the zero-expectation level (i.e., the anticipated amplitude in the absence of source emission). In each panel the solid line indicates the best fit model for the given species from Jørgensen *et al.* (2004b, 2005c) (constant abundance for SO and  $\text{H}^{13}\text{CN}$  and jump abundance for  $\text{CH}_3\text{OH}$ ), the dashed-dotted lines indicate envelope models with an additional disk component with a Gaussian brightness distribution (FWHM of 200 AU). The dashed lines indicate additional models: for SO models with abundance enhancements in the inner regions by factors 10 (dark) and 100 (light). For  $\text{H}^{13}\text{CN}$  models with a drop abundance profile and for  $\text{CH}_3\text{OH}$  a model with a jump in abundance corresponding to a hot corino. The **right column** shows the corresponding abundance profiles for the three species (dashed lines) and the temperature profile for NGC 1333-IRAS2A (solid line). For further details see Jørgensen *et al.* (2005a).

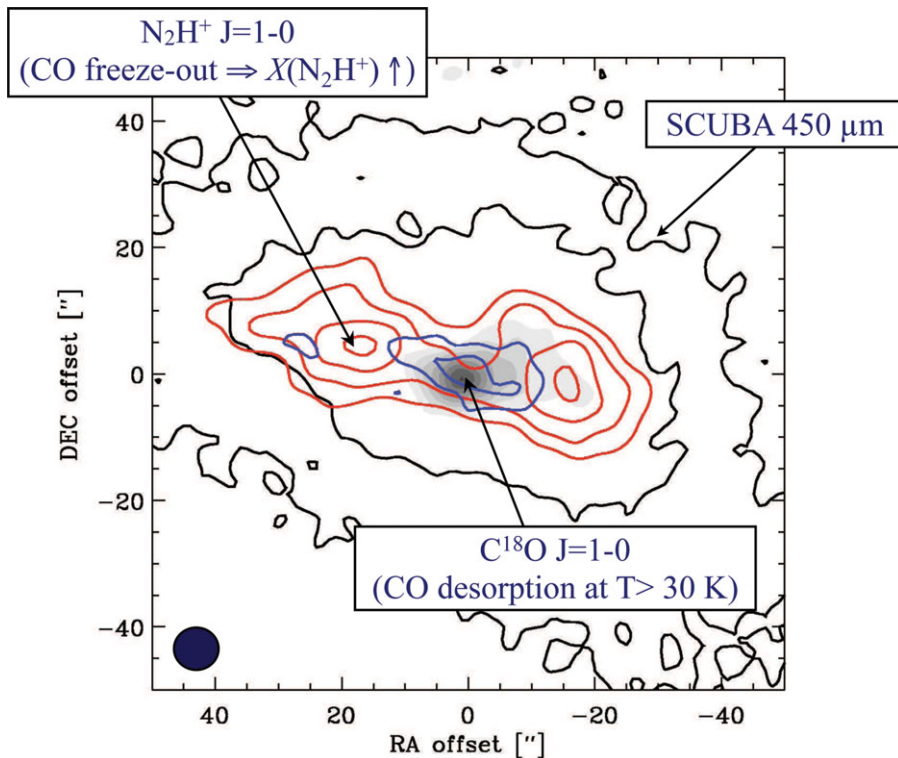


**Figure 6.** Morphology of the L483 protostellar core in 450  $\mu\text{m}$  continuum from JCMT/SCUBA observations as well as  $\text{N}_2\text{H}^+$  1–0 and  $\text{C}^{18}\text{O}$  1–0 from observations with the Owens Valley Radio Observatory Millimeter Array (for further details see Jørgensen 2004). The 450  $\mu\text{m}$  observations show the overall (asymmetric) distribution of dust in the core. The  $\text{C}^{18}\text{O}$  emission is only present at the center where CO evaporates of the dust grains at temperatures of 30 K, whereas  $\text{N}_2\text{H}^+$  predominantly is present at larger scales where CO is frozen out. Adapted from Jørgensen (2004).

temperatures above 100 K by the radiation from the newly formed protostars. Until now, four of these “hot corinos” have been suggested to be present toward the low-mass protostars, IRAS 16293-2422, NGC 1333-IRAS2A, NGC 1333-IRAS4A and NGC 1333-IRAS4B, based on single-dish observations of the before mentioned complex organics and through modeling of  $\text{H}_2\text{CO}$  and  $\text{CH}_3\text{OH}$  observations (e.g., Ceccarelli *et al.* 2000; Schöier *et al.* 2002; Maret *et al.* 2005). The hot corinos themselves, however, are severely diluted in single-dish beams ( $\lesssim 100$  AU sizes, compared to typical single-dish telescope beams of 1000–2000 AU). The interpretation of single-dish observations and comparison to models therefore relies on extrapolation of the density and temperature distribution from observations on larger scales that as pointed out are highly uncertain on the  $\lesssim 100$  AU scales where the hot corino activity may take place. There are therefore good reasons to push to high angular resolution.

Studies targeting lines of  $\text{CH}_3\text{OH}$  and  $\text{H}_2\text{CO}$  have highlighted the problems in separating the emission from outflows and possible hot corinos (Jørgensen *et al.* 2007; Schöier *et al.* 2004). The main, medium excitation ( $E_u = 50$  K and above) transitions of  $\text{H}_2\text{CO}$  and  $\text{CH}_3\text{OH}$  in the 300 GHz windows are strongly affected by compact outflow emission up to  $10''$  scales. For the more complex organic molecules, the picture at first glance appears simpler: for the four well-studied hot corinos images of the complex organic molecules show relatively compact emission with extents comparable to the typical



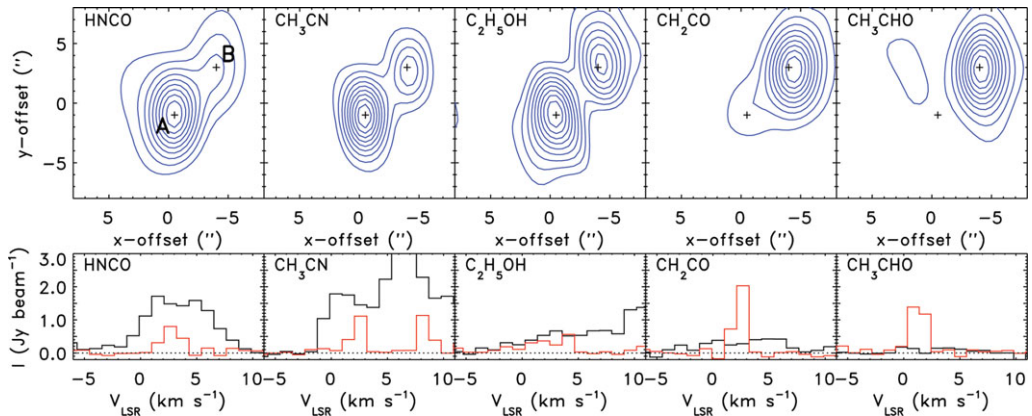


**Figure 7.** Observations of complex organics toward the IRAS 16293-2422 binary system (Bisschop *et al.* 2008; Jørgensen *et al.* 2011).

synthesized beam sizes of about  $1''$  (200 AU). As an example, high angular resolution interferometer observations of IRAS 16293-2422 (Bottinelli *et al.* 2004; Kuan *et al.* 2004; Bisschop *et al.* 2008), show that line emission of the organic molecules peaks close to the position of two compact dust continuum peaks indicating the locations of the central protostars (Fig. 7) – although the relative strengths of the complex organics differ between the two sources. However, low surface brightness emission from many other species, not necessarily associated with the hot corinos, at first glance also shows similar compact morphologies with deconvolved sizes comparable to the current interferometers' typical angular resolution (Jørgensen *et al.* 2007, 2011). Also, as pointed out by Chandler *et al.* (2005) from their subarcsecond observations of IRAS 16293-2422, there are small offsets of order  $0.1''$  between the location of the dust and the peaks of the complex organics, which is now also seen for the three other hot corino sources (Persson *et al.* 2011). Chandler *et al.* (2005) argued that these offsets (and similar offsets for high excitation transitions of non-organic molecules) reflected the action of shocks related to the protostellar jets rather than the passive (thermal) heating by the central protostars.

Another possibility, namely that many of these species reside in the circumstellar disks, has been prompted by recent subarcsecond millimeter wavelength resolution observations of a line of the water isotopologue,  $\text{H}_2^{18}\text{O}$ , at 203.4 GHz (1.4 mm) using the IRAM Plateau de Bure Interferometer (PdBI; Jørgensen & van Dishoeck) as well Spitzer Space Telescope detections of water at mid-infrared wavelengths (Watson *et al.* 2007) toward the deeply embedded protostar NGC 1333-IRAS4B. Because of the high densities required to excite the mid-infrared lines, the Spitzer Space Telescope detections were interpreted as signs of an ongoing accretion shock in the circumstellar disk. The IRAM PdBI observations confirmed that the water has its origin in the inner 25 AU (radius) of the disk predicted on basis of models of the Spitzer observations – and furthermore showed a tentative velocity gradient perpendicular to the propagation direction of the outflow probed by high angular resolution CO and maser observations. Similar high angular resolution ground-based detections of the  $\text{H}_2^{18}\text{O}$  203.4 GHz transition toward three other hot corino candidates (Persson *et al.* 2011; and M. Persson *et al.*, in prep.), suggests that this source is not unique. The simultaneous detections of complex organic species on similar scales supports the basic idea that the release of complex organics is prompted by the evaporation of water-rich ice mantles in these systems.

### 3.3. Chemistry of 100 AU regions

No matter the physical origin of the complex organic molecules and water, the interferometric observations show that they are present on few hundred scales. In their SMA study of IRAS 16293-2422 Bisschop *et al.* (2008) found strong chemical differentiation of the observed complex organic molecules between the two components in the binary system (Fig. 7): the nitrogen-bearing species HNC and CH<sub>3</sub>CN were detected toward both components in the binary but much stronger in the “A” source where the opposite was found to be the case for the oxygen-bearing species, C<sub>2</sub>H<sub>5</sub>OH, CH<sub>2</sub>CO and CH<sub>3</sub>CHO – the latter only seen toward the “B” source. Likewise, Persson *et al.* (2011) used millimeter interferometric observations of the H<sub>2</sub><sup>18</sup>O isotopologue to trace the abundances of a few complex organics relative to water in the warm inner regions of three other low-mass hot corinos in NGC 1333. They also found differences in the abundances of, e.g., C<sub>2</sub>H<sub>5</sub>CN and CH<sub>3</sub>OCH<sub>3</sub> relative to water: while the latter is relatively constant between the three different sources, the C<sub>2</sub>H<sub>5</sub>CN to water abundance ratio varies by orders of magnitude. Similar differences between oxygen- and nitrogen-bearing species have also been seen in other types of star-forming regions (e.g., the sample of high-mass stars surveyed by Bisschop *et al.* 2007). As discussed by Bisschop *et al.* (2008), these differences can be explained through differences in their formation on grain surfaces and, e.g., the initial ice compositions. Differences between the oxygen bearing species also suggest that simple successive hydrogenation reactions on the grain surfaces are insufficient to explain the observed gas-phase abundances.

The H<sub>2</sub><sup>18</sup>O observations also makes it possible to revisit a long-standing discussion concerning the astrochemistry of water – namely what is the deuteration of water. It is thought that the amount of deuterated relative to non-deuterated water is established in these icy grain mantles. Determining exactly when this ratio is established and how it varies, is an important for understanding, e.g., whether water undergoes significant processing in warm regions of protostellar envelopes or disks.

Multi-transition HDO and H<sub>2</sub>O single-dish observations from ground- and space-based observations have previously been used to estimate the HDO/H<sub>2</sub>O abundance ratios in low-mass protostellar envelopes (e.g., Stark *et al.* 2004; Parise *et al.* 2005; Liu *et al.* 2011). Despite the advantages offered by the ranges of excitation conditions probed by the multi-transitions observations, these studies are still complicated by the relatively large beam sizes of the ground-based single-dish and space observatories and are therefore strongly dependent on exact line radiative transfer models utilized for the interpretation. In particular, the H<sub>2</sub>O abundance is highly uncertain: even recent Herschel observations are predominantly sensitive to the impact of outflows and shocks on larger scales and only provide upper limits on the water abundance in the inner protostellar envelopes (e.g., Kristensen *et al.* 2010), although recent Herschel observations of H<sub>2</sub><sup>18</sup>O toward low-mass protostars (e.g., R. Visser *et al.*, in prep) may alleviate some of these problems.

Ground-based interferometric observations make it possible to directly measure the HDO/H<sub>2</sub>O abundance ratio in the warm gas close to the central protostars. A non-detection of the HDO 3<sub>12</sub> – 2<sub>21</sub> transition at 225.9 GHz toward NGC 1333-IRAS4B from the SMA together with the detected 203.4 GHz transition of H<sub>2</sub><sup>18</sup>O for example put a strong 3σ upper limit of 6×10<sup>-4</sup> to the HDO/H<sub>2</sub>O ratio on scales of a few hundred AU, thus implying that the ratio is not enhanced above the cometary value. A detection of both the H<sub>2</sub><sup>18</sup>O 203.4 GHz and HDO 225.9 GHz transition toward the “A” component in IRAS 16293-2422 (M. Persson *et al.*, in prep.) likewise suggests an HDO/H<sub>2</sub>O abundance ratio of 1–2×10<sup>-3</sup> – only slightly enhanced above the cometary value. Higher sensitivity (multi-transition) H<sub>2</sub><sup>18</sup>O and HDO observations with ALMA for more sources are needed

to settle this issue. However, to target the 203.4 GHz  $\text{H}_2^{18}\text{O}$  transition with this sensitivity the full complement of ALMA band-5 receivers will be necessary.

#### 4. Outlook: on to ALMA

Clearly many of the above issues will be addressed with the coming of the Atacama Large Millimeter Array that at the writing of this proceedings paper just had its deadline for “cycle 0” proposals. The main features of ALMA are:

- *Its high sensitivity* due to the excellent site, state-of-the-art technology and, in particular, large collecting area. This will allow studies of rare molecular species, isotopologues as well as faint lines that selectively probe specific components in the protostellar environments.
- *Its high angular resolution* with baselines out to 16 km will resolve structures down to few AU scales in the centers of protostars, including the forming circumstellar disks and their physical and chemical structures.
- *Its imaging capabilities* with the large number of antennae that will provide broad  $(u, v)$  coverage even in relatively short observations and thereby not be as affected by spatial filtering (resolving out of large-scale smooth structures) or dynamical range as current interferometers. This will in particular be key for imaging the few hundred AU scales of protostellar envelopes understanding, e.g., the interactions between the protostellar outflows and envelopes – or putting hard constraints on the radial variations of molecular species.

Of course, designing feasible programs fully utilizing the promise of ALMA requires some thought. For example, the highest angular resolution will only be achievable for the brightest lines – some of which will be optically thick on large scales and thus provide limited information. Thus, particular care needs to be taken to pick the optimal balance between achievable angular resolution/sensitivity and the posed questions. Also, there are many reasons to expect that the protostars will show significantly more complex structures than what is captured by for example traditional models for protostellar cores, pushing the need to even more sophisticated modeling tools. Still, this is of course a challenge in itself, and for anyone up to it, it is clear that ALMA will provide great possibilities for comprehensive molecular imaging studies of protostellar systems (as well as many other types of sources) that will keep astrochemists busy for years to come.

#### References

- Basu, S. 1998, *ApJ*, 509, 229
- Bisschop, S. E., Jørgensen, J. K., Bourke, T. L., Bottinelli, S., & van Dishoeck, E. F. 2008, *A&A*, 488, 959
- Bisschop, S. E., Jørgensen, J. K., van Dishoeck, E. F., & de Wachter, E. B. M. 2007, *A&A*, 465, 913
- Bottinelli, S., Ceccarelli, C., Neri, R., *et al.* 2004, *ApJ*, 617, L69
- Brinch, C., Crapsi, A., Jørgensen, J. K., Hogerheijde, M. R., & Hill, T. 2007, *A&A*, 475, 915
- Brinch, C., Jørgensen, J. K., & Hogerheijde, M. R. 2009, *A&A*, 502, 199
- Cazaux, S., Tielens, A. G. G. M., Ceccarelli, C., *et al.*, 2003, *ApJ*, 593, L51
- Ceccarelli, C., Loinard, L., Castets, A., Tielens, A. G. G. M., & Caux, E. 2000, *A&A*, 357, L9
- Chandler, C. J., Brogan, C. L., Shirley, Y. L., & Loinard, L. 2005, *ApJ*, 632, 371
- Chiang, H.-F., Looney, L. W., Tassis, K., Mundy, L. G., & Mouschovias, T. C. 2008, *ApJ*, 680, 474
- Enoch, M. L., Corder, S., Duchene, G., *et al.*, 2011, ArXiv e-prints
- Enoch, M. L., Corder, S., Dunham, M. M., & Duchêne, G. 2009, *ApJ*, 707, 103

- Galli, D. & Shu, F. H. 1993a, *ApJ*, 417, 220  
 Galli, D. & Shu, F. H. 1993b, *ApJ*, 417, 243  
 Hennebelle, P. & Ciardi, A. 2009, *A&A*, 506, L29  
 Ivezić, Ž., Nenkova, M., & Elitzur, M. 1999, User Manual for DUSTY, University of Kentucky Internal Report  
 Jørgensen, J. K. 2004, *A&A*, 424, 589  
 Jørgensen, J. K., Bourke, T. L., Myers, P. C., *et al.*, 2007, *ApJ*, 659, 479  
 Jørgensen, J. K., Bourke, T. L., Myers, P. C., *et al.*, 2005a, *ApJ*, 632, 973  
 Jørgensen, J. K., Bourke, T. L., Nguyen Luong, Q., & Takakuwa, S. 2011, *Å*, submitted  
 Jørgensen, J. K., Harvey, P. M., Evans, N. J. I., *et al.*, 2006, *ApJ*, 645, 1246  
 Jørgensen, J. K., Hogerheijde, M. R., van Dishoeck, E. F., Blake, G. A., & Schöier, F. L. 2004a, *A&A*, 413, 993  
 Jørgensen, J. K., Schöier, F. L., & van Dishoeck, E. F. 2002, *A&A*, 389, 908  
 Jørgensen, J. K., Schöier, F. L., & van Dishoeck, E. F. 2004b, *A&A*, 416, 603  
 Jørgensen, J. K., Schöier, F. L., & van Dishoeck, E. F. 2005b, *A&A*, 435, 177  
 Jørgensen, J. K., Schöier, F. L., & van Dishoeck, E. F. 2005c, *A&A*, 437, 501  
 Jørgensen, J. K. & van Dishoeck, E. F. 2010, *ApJ*, 710, L72  
 Jørgensen, J. K., van Dishoeck, E. F., Visser, R., *et al.*, 2009, *A&A*, 507, 861  
 Kristensen, L. E., Visser, R., van Dishoeck, E. F., *et al.*, 2010, ArXiv e-prints  
 Kuan, Y., Huang, H., Charnley, S. B., *et al.*, 2004, *ApJ*, 616, L27  
 Liu, F., Parise, B., Kristensen, L., *et al.*, 2011, *A&A*, 527, A19  
 Lommen, D., Jørgensen, J. K., van Dishoeck, E. F., & Crapsi, A. 2008, *A&A*, 481, 141  
 Maret, S., Ceccarelli, C., Tielens, A. G. G. M., *et al.*, 2005, *A&A*, 442, 527  
 Matthews, B. C., Hogerheijde, M. R., Jørgensen, J. K., & Bergin, E. A. 2006, *ApJ*, 652, 1374  
 Maury, A. J., André, P., Hennebelle, P., *et al.*, 2010, *A&A*, 512, A40  
 Parise, B., Caux, E., Castets, A., *et al.*, 2005, *A&A*, 431, 547  
 Persson, M., Jørgensen, J. K., & van Dishoeck, E. F. 2011, *A&A*, submitted  
 Sakai, N., Sakai, T., & Yamamoto, S. 2006, *PASJ*, 58, L15  
 Schöier, F. L., Jørgensen, J. K., van Dishoeck, E. F., & Blake, G. A. 2002, *A&A*, 390, 1001  
 Schöier, F. L., Jørgensen, J. K., van Dishoeck, E. F., & Blake, G. A. 2004, *A&A*, 418, 185  
 Shirley, Y. L., Evans, N. J., & Rawlings, J. M. C. 2002, *ApJ*, 575, 337  
 Stark, R., Sandell, G., Beck, S. C., *et al.*, 2004, *ApJ*, 608, 341  
 Terebey, S., Shu, F. H., & Cassen, P. 1984, *ApJ*, 286, 529  
 van der Tak, F. F. S., Black, J. H., Schöier, F. L., Jansen, D. J., & van Dishoeck, E. F. 2007, *A&A*, 468, 627  
 Watson, D. M., Bohac, C. J., Hull, C., *et al.*, 2007, *Nature*, 448, 1026

## Discussion

MAUERSBERGER: H<sub>2</sub>O has a complex spectrum and the lines you were observing are high in the excitation ladder. How much are your abundance estimations influenced by masing?

JØRGENSEN: This is an important issue indeed. In the specific cases of the IRAM Plateau de Bure observations, we actually have evidence that the H<sub>2</sub><sup>18</sup>O transition is not severely by masing – for example that the widths of the observed H<sub>2</sub><sup>18</sup>O lines are very close to those of other species. Also, species-to-species variations in the line strengths are much smaller than the source-to-source variations.